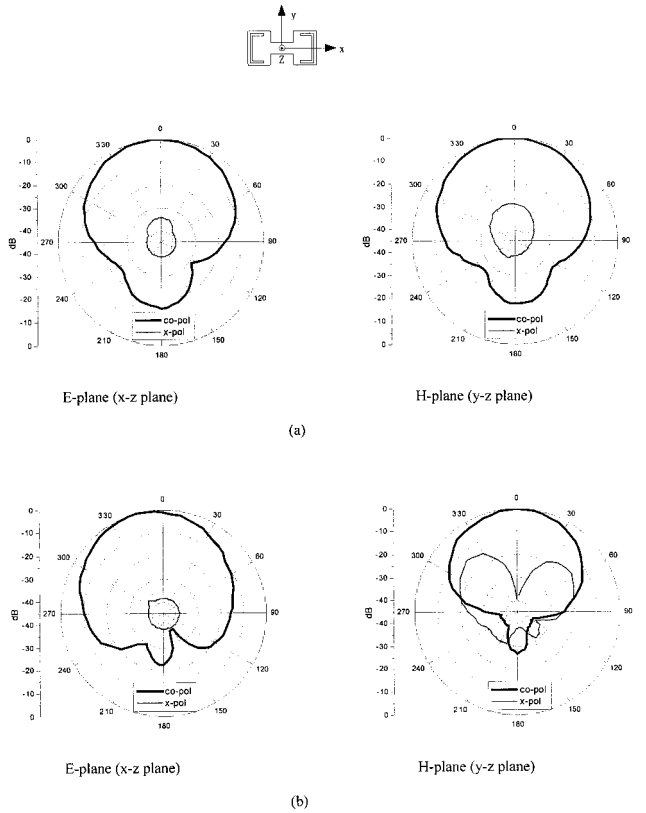

Figure 4 Measured radiation patterns at two operating frequencies of the antenna: (a) $f_{10} = 929$ MHz; (b) $f_{30} = 1790$ MHz

REFERENCES

1. S. Maci, G.B. Gentili, P. Piazzesl, and C. Salvador, Dual-band slot-loaded patch antenna, IEE Proc Microwave Antennas Propagat 142 (1995), 225–232.
2. Y.X. Guo, K.M. Luk, and K.F. Lee, A dual-band patch antenna with two U-shaped slots, Microwave Opt Technol Lett 26 (2000), 73–75.
3. K.L. Wong and J.Y. Sze, Dual-frequency slotted rectangular microstrip antenna, Electron Lett 34 (1998), 1368–1370.
4. V. Palanisamy and R. Garg, Rectangular ring and H-shaped microstrip antenna—Alternatives to rectangular patch antenna, Electron Lett 21 (1985), 874–876.
5. S.C. Gao, L.W. Li, T.S. Yeo, and M.S. Leong, A dual-frequency small microstrip antenna, Antennas Propagat Symp 4 (2001), 86–89.

AN OMNIDIRECTIONAL ADE REFLECTOR ANTENNA

José R. Bergmann[1] and Fernando J. S. Moreira[2]
[1] CETUC–Center for Telecommunications Studies
Catholic University of Rio de Janeiro
Rio de Janeiro
RJ 22453-900, Brazil
[2] Department of Electronics Engineering
Federal University of Minas Gerais
Belo Horizonte, MG 30161-970, Brazil

Received 7 July 2003

ABSTRACT: *In this work, an axially-displaced-ellipse (ADE) dual-reflector antenna for the achievement of an omnidirectional coverage is proposed. Its geometry is briefly presented and some relevant features are compared against previously suggested reflector antennas, designed for the same purpose. The present ADE configuration is capable of yielding the desired aperture illumination with relatively smaller reflector dimensions, thus providing a compact arrangement suited for use at base stations of point-to-multi-point radio links. Numerical simulations are presented to illustrate the usefulness and advantages of the proposed reflector antenna.* © 2004 Wiley Periodicals, Inc. Microwave Opt Technol Lett 40: 250–254, 2004; Published online in Wiley InterScience (www.interscience.wiley.com). DOI 10.1002/mop.11344

Key words: *dual reflector antennas; omnidirectional antennas*

1. INTRODUCTION

Some of the future generations of communication systems are expected to provide services through high-data-rate wireless channels. They will operate at the Ka and millimeter-wave bands, which provide the broad frequency bands required for these services (LMDS, MVDS, and so on). Compared to other technologies, broadband wireless access is emerging as a technology that offers rapid deployment, higher scalability, and lower maintenance, cable, and upgrade costs. The use of relatively higher frequencies (up to millimeter waves) makes the employment of compact reflector antennas, capable of providing the wider absolute bandwidths necessary to transmit wideband signals, an attractive method.

A circularly symmetric dual-reflector antenna, investigated in [1, 2], is suitable for vertical polarization and omnidirectional coverage in the azimuthal plane. The antenna consists of a parabolic subreflector and a conical main reflector fed by a coaxial horn designed to transmit only the fundamental TEM mode. Such configuration is herein defined as a paraboloid plus cone (PACO). For different antenna polarizations, feed horns radiating TM_{01} or TE_{01} modes are also applied. In [2], geometrical optics (GO) was employed to shape both reflectors in order to control the phase and power at the antenna aperture to achieve higher gains. Alternatively, a single circularly-symmetric shaped reflector configuration fed by a coaxial conical horn was investigated in [3]. The reflector surface was shaped to attain a cosecant squared-like power pattern in the vertical plane to account for free-space attenuation, while concentrating the radiated energy below the horizon for reduced interference. As compared to the omnidirectional dual-reflector antenna, the major disadvantage of the single-reflector system is the large reflector diameter required to achieve the necessary aperture width for adequate control of the vertical radiation pattern.

This work was partially supported by CNPq under Covenant PRONEX 664041/1996-S and Projects 462669/00-9, 470495/2001-4, and 551990/2002-2, and by FAPEMIG under Project TEC 659/98.

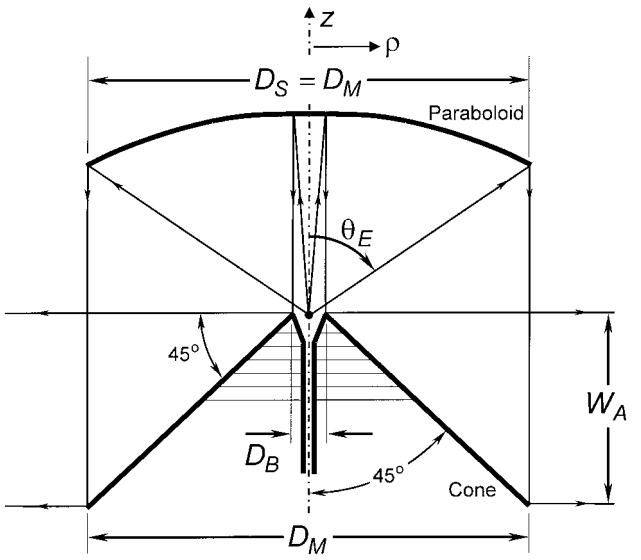

Figure 1 Basic features of the PACO geometry

In the present work, a novel circularly symmetric dual-reflector antenna is suggested for the desired omnidirectional coverage. The reflector system is based on the axially-displaced ellipse (ADE) configuration, extensively discussed in [4]. The ADE consists of circularly symmetric sub- and main-reflectors generated by an ellipse and a parabola, respectively. One of the major features of the omnidirectional ADE is the presence of a real ring caustic between the reflectors, which ends up minimizing the subreflector radiation toward the feed horn (thus reducing the feed return loss) while enabling a larger aperture width with relatively smaller reflector diameters (desirable for compact-antenna applications).

In order to establish the superior performance of the ADE for omnidirectional coverage, this work is organized as follows. In section 2, some of the most relevant features of the PACO antenna are briefly presented. The same is done for the ADE in section 3, with a special emphasis on the associate novel features. Both antennas are then designed for 10-dBi gain and their radiation patterns numerically determined by the method of moments (MoM) in section 4. This section also presents MoM results for the VSWR behavior inside the feed's waveguide across a $\pm 10\%$ bandwidth, which will clearly demonstrate the better performance of the ADE configuration. The work is concluded in section 5.

2. PACO GEOMETRY

The PACO geometry is relatively simple under a geometrical optics perspective [1]. However, some brief comments are in place in order to establish some useful geometrical parameters, which will also be adopted for the ADE in section III and will permit an appropriate comparison between the antennas. The PACO is illustrated in Figure 1, where D_M and D_S are the main- and subreflector diameters, respectively, D_B is the diameter of the main-reflector central aperture (enabling the feed access to the focus of the dual-reflector system), W_A is the width of the cylindrical aperture, and θ_E is the subreflector edge angle. It is clear from Figure 1 that the paraboloid focal length F provides the distance from the system focus to the subreflector vertex. Also, from the paraboloid equation, $\tan(\theta_E/2) = D_S/(2F)$, with $D_S = D_M$ being a particular feature of the PACO antenna (see Fig. 1). The main-reflector cone is specified with an internal semi-angle of 45° to provide a right angle between the output rays and the axis of symmetry (the z axis). So, for the PACO antenna, $2\,W_A = D_M - D_B$ and, consequently, $W_A/D_M < 1/2$. The system is fed by a coaxial feed horn that provides a vertically polarized radiation with phase-center located very close to the horn's aperture. In the present work, both the PACO and the ADE are specified such that the focal point of the reflector system is always at the center of the main-reflector central aperture (see Fig. 1).

3. THE OMNIDIRECTIONAL ADE GEOMETRY

A novel omnidirectional ADE antenna (herein defined as the OADE) is proposed. Its geometry is based on the classical ADE dual-reflector configuration, which is detailed discussed in [4]. The OADE configuration in the vertical plane is depicted in Figure 2, where D_M, D_S, D_B, W_A, and θ_E are as described in section 2. Invoking GO principles, the ADE provides (as does the PACO), a cylindrical aperture with a uniform phase distribution. To achieve this, the sub- and main-reflectors are generated by an ellipse and a parabola, respectively. One of the ellipse foci O is placed at the symmetry axis, defining the focus of the dual-reflector system. The other focus P coincides with the parabola focus and will define the ring caustic laying between the sub- and main-reflectors. The parabola is rotated such that its axis makes a right angle with the symmetry axis. The 3D reflector surfaces are then obtained by spinning both generating conic sections about the symmetry axis (see Fig. 2). Consequently, the main-reflector has a small circular aperture at its center (with diameter D_B), which enables the feed access to the focal point O. As for the PACO, the OADE will be specified with O at the center of the main-reflector central aperture (see Fig. 2).

The many advantages of the OADE with respect to the PACO basically rely on the presence of a real ring caustic between the reflectors. For instance, this enables the adjustment of the generating conic sections in order to place the parabola focus P away from the symmetry axis, while enforcing a small angle between the parabola and ellipse axes. That provides two options for the designer: an elongated parabola and, consequently, a larger W_A/D_M ratio than the PACO antenna or about the same W_A/D_M of the PACO, but with a smaller D_S. Furthermore, the OADE also provides a larger concavity for the subreflector, thus reducing the feed's spillover. Finally, as can be seen from Figure 2, the subreflector scattering toward the horn's aperture is considerably reduced.

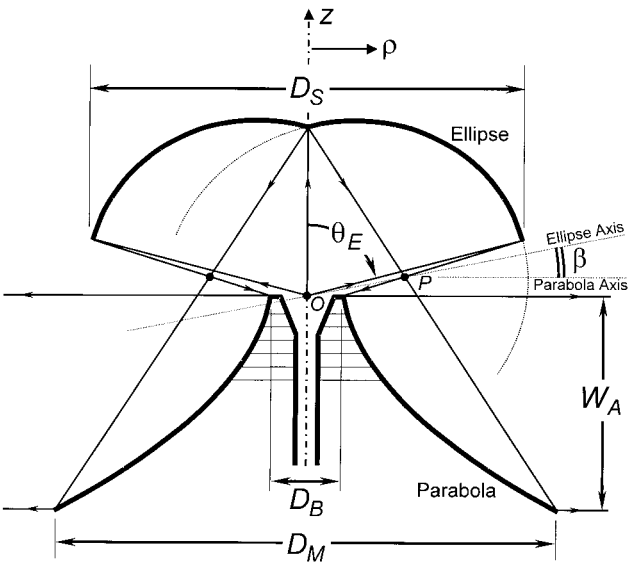

Figure 2 The OADE geometry

In order to uniquely achieve an OADE reflector system, four parameters must be specified: the parabola focal length F, the ellipse eccentricity e, inter-focal distance $2c$, and the angle β between the ellipse and the parabola axes. As these are not appropriate input parameters for a practical design, four other parameters are chosen instead: D_S, D_B, W_A, and θ_E (D_M is connected with these parameters). One can obtain the conics' characteristics from the four input parameters with the help of the polar equations of the parabola and ellipse, following a procedure similar to that in [4] but with the parabola axis tilted by 90°.

Some parametric studies were conducted to establish the geometrical conditions for a large W_A/D_M ratio, always enforcing $D_M \geq D_S$. It was observed that, in general, a large W_A/D_M ratio is accomplished when D_S is considerably smaller than D_M, $\theta_E \rightarrow 90°$ (close enough while yielding the desired subreflector clearance), and D_B as small as possible (just to enable the feed access). Under the same conditions, but reducing W_A in order to achieve the same W_A/D_M of the PACO, one ends up with an OADE with a smaller D_S.

4. ANTENNA DESIGNS AND ANALYSES

In this section, the electrical performances of the PACO and OADE configurations are investigated. As a reference for a comparative study, both antennas were designed to occupy approximately the same volume. Their geometries in the vertical plane (and in scale) are depicted in Figures 3(a) and (b), where all dimensions are given in wavelengths (λ) at an arbitrary central frequency f_C. Both antennas were also designed to provide a peak gain of about 10 dBi at the horizontal plane ($\theta = 90°$) at f_C. Consequently, both antennas ended up with $D_B = 2.4\lambda$, $W_A = 7.5\lambda$, $\theta_E = 75°$, $D_M \approx 17\lambda$, and $H \approx 13\lambda$, where H is the antenna height. Note that both antennas have $W_A/D_M \approx 0.43$; but the OADE has a smaller subreflector ($D_S = 14.5\lambda$) than the PACO ($D_S = 17\lambda$), while providing approximately the same 2λ clearance for the cylindrical aperture. The parabola of the PACO's subreflector has a focal distance of 5.5λ, while for the OADE $F = 2.18\lambda$, $2c = 3.4\lambda$, $e = 0.292$, and $\beta = 11.6°$.

In order to achieve the desired vertical polarization, both antennas are fed by a coaxial horn with a quarter-wave choke placed at the horn's aperture plane, as indicated in Figure 3 (where the inner conductor of the coaxial horn is not shown). This is the same horn used in [3], for which measured patterns are available. The horn is fed by a coaxial waveguide designed to propagate only the fundamental TEM mode. Consequently, the horn's radiation has an omnidirectional pattern with a null along the symmetry axis (a doughnut-like main lobe, as depicted in Fig. 4). The quarter-wave choke was implemented to minimize the feed back-scattering and, consequently, its interference in the antenna radiation pattern below the horizon. Measurements indicate that the choke allows a reduction in the side-lobe levels larger than 10 dB.

The present OADE configuration not only provides a dual-reflector system with a smaller D_S but also achieves a lower feed return-loss performance across the operation band (±10% from the central frequency f_C). To properly demonstrate this phenomenon, the electromagnetic analysis must account for second order effects resulting from feed and reflector interaction, specially in these compact reflector arrangements (see Fig. 3). Hence, a method of moments (MoM) analysis was employed, based in [5]. An equivalent distribution of electric and magnetic current sources was used to excite only the fundamental TEM mode toward the waveguide-horn junction. To absorb the TEM propagation in the opposite direction and, consequently, establish the feed return loss, a surface impedance was placed at the end of the coaxial

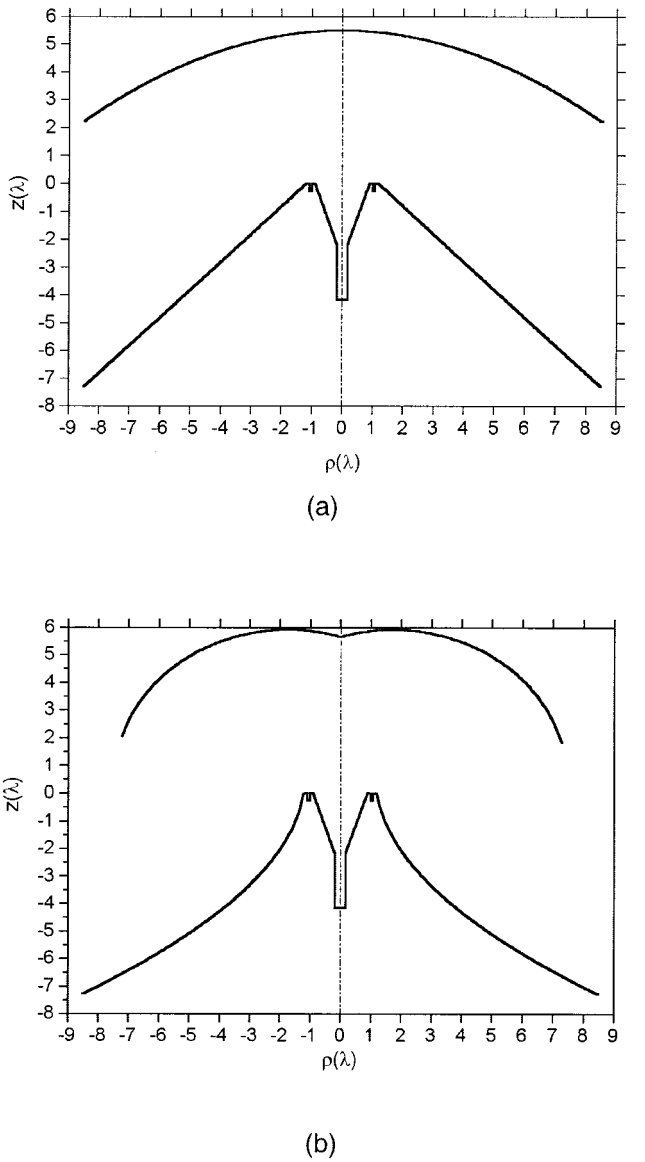

Figure 3 Scaled geometries of the 10-dBi (a) PACO and (b) OADE antennas in the vertical plane

waveguide [5]. The inclusion of the reflector surfaces in the MoM analysis was quite straightforward. Initially, the MoM was applied to predict the feed far-field pattern for comparison with measured data. The results are depicted in Figure 4 at the operation-band extremes ($0.9\ f_C$ and $1.1\ f_C$), thus demonstrating the efficiency and robustness of the adopted MoM analysis.

From Figure 4 one can inspect that the doughnut-like feed pattern contracts toward the symmetry axis as frequency and, consequently, that the aperture's electrical dimensions increase, intensifying the illumination of the central portion of the subreflector. Consequently, for the PACO configuration, the subreflector radiation toward the horn's aperture increases with frequency, thus yielding a large electromagnetic interaction between the feed and the subreflector, which ultimately produces a large and highly oscillatory feed return-loss across the operation band, as observed in [2] after measurements. The same radiation mechanism also provides a large illumination of the discontinuity at the junction between the horn and main-reflector, which, in consequence, increases the antenna side-lobe levels. For the OADE, however, the

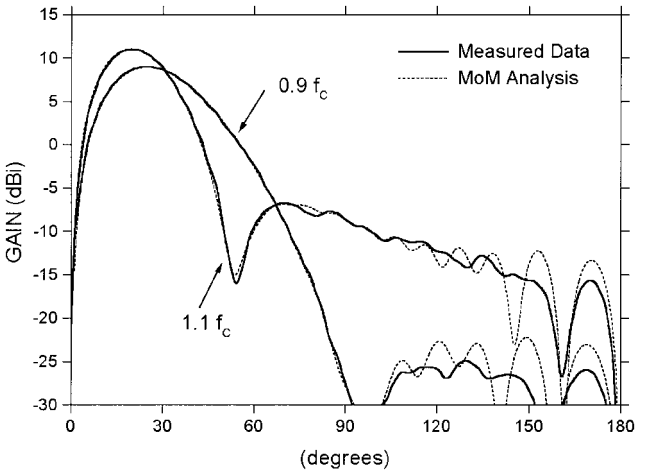

Figure 4 Radiation patterns of the coaxial horn at 0.9 f_C and 1.1 f_C: measured data and MoM analysis.

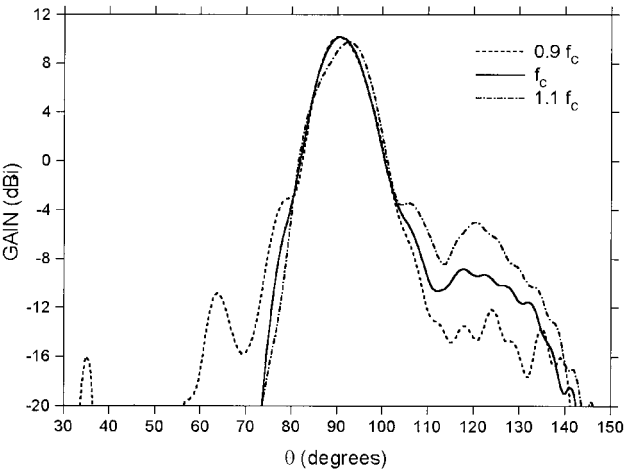

Figure 6 Radiation patterns of the PACO antenna at 0.9 f_C, f_C, and 1.1 f_C: MoM analysis

radiation departing from the subreflector's vertex is directed toward the farthest main-reflector's rim (see Fig. 2) and all those phenomena previously described will have relatively smaller impact. So, it is anticipated that the OADE, when compared with the PACO, has a smaller and quasi-uniform return loss across the band, together with a radiation pattern with lower side-lobe levels.

To demonstrate the previous assertions, MoM analyses were conducted to estimate the return loss inside the coaxial waveguide across the operation band for the feed horn alone, for the PACO antenna, and for the OADE. The results are shown in Figure 5. The feed horn was designed to provide a return loss lower than -16 dB over a $\pm 10\%$ bandwidth about the central frequency f_C, as depicted in Figure 5. When this horn is applied to excite the present OADE, the overall antenna return loss has quite the same behavior as the horn alone (see Fig. 5), indicating that the subreflector scattering toward the horn's aperture has negligible influence upon the return loss. However, for the PACO antenna, this influence is quite considerable, as Figure 5 indicates. From this figure, one observes two nulls in the PACO's return loss: at $f/f_C = 0.97$ and 1.06. As the distance between the horn's aperture and the paraboloid vertex is about 5.5λ at f_C [see Fig. 3(a)], the frequency range between these nulls corresponds to a half-wavelength variation in that electrical distance, confirming that the oscillatory behavior of the PACO's return loss is truly due to the electromagnetic interaction between the horn and the paraboloidal subreflector. Also, from Figure 5 one observes that the peaks of the PACO's return loss increase with frequency, which is a consequence of the contraction of the doughnut-like feed pattern (see Fig. 4) that ultimately intensifies the subreflector radiation toward the horn, as anticipated.

Furthermore, MoM analyses were also conducted for the evaluation of the radiation patterns of the PACO and OADE antennas. The results are presented in Figures 6 and 7, respectively, for the central and limiting frequencies of the operation band. First of all, one observes that the radiation peaks present a small angular tilt about the horizon line ($\theta = 90°$), which is caused by a nonuniform phase distribution over the main-reflector cylindrical aperture. That is because the optical properties of these compact antenna configurations suppose that the subreflector is illuminated by a spherical wavefront in order to obtain a uniform phase at the antenna aperture. As the subreflector is in the feed's near-field region (see Fig. 3), the nonspherical phase front is incident upon the subreflector shifts, thus generating an asymmetric radiation pattern in the elevation plane. Although the peak gain is approximately the same (10 dBi) for both

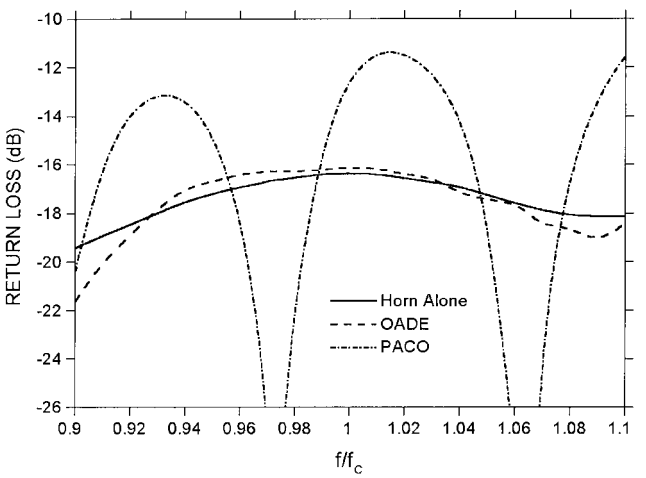

Figure 5 Return loss across the operation band for the horn alone, OADE, and PACO

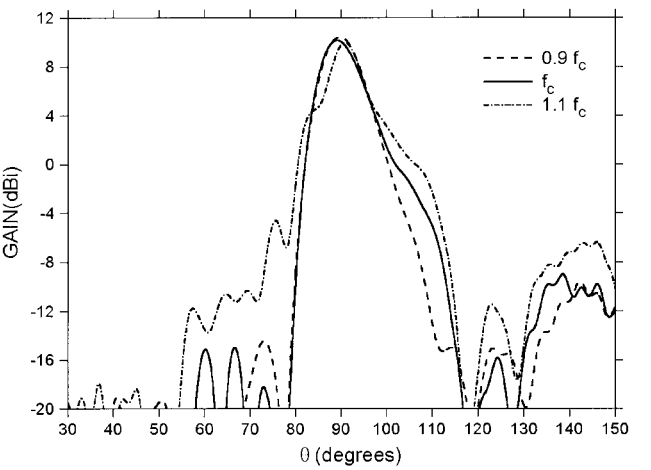

Figure 7 Radiation patterns of the OADE antenna at 0.9 f_C, f_C, and 1.1 f_C: MoM analysis

antennas, for the PACO the peak is tilted about one degree below the horizon (see Fig. 6). For the OADE, however, the reverse of the subreflector radiation by the real ring caustic tilts the peak one degree in the opposite sense (see Fig. 7).

The contraction of the feed doughnut-like radiation pattern affects also the antenna radiation by increasing the illumination of the discontinuity at the main-reflector-horn junction, by bringing some sidelobes to illuminate the subreflector and, consequently, by underilluminating and increasing the phase variation over the antenna cylindrical aperture. Figures 6 and 7 show that, although the antenna aperture becomes electrically smaller, at the lower limit of the band ($0.9\,f_C$) the gain is kept approximately constant as the feed radiation pattern broads and, consequently, produces a more uniform illumination over the antenna aperture.

5. CONCLUSION

This work has presented a novel axis-displaced-ellipse dual-reflector antenna for omnidirectional coverage (OADE). When compared with the usual paraboloid-cone dual-reflector antenna (also designed to provide an omnidirectional radiation pattern), the OADE results in a more compact configuration with the additional advantage of lower return-loss levels. Several numerical analyses based on the MoM were conducted for both antennas over a $\pm 10\%$ bandwidth, demonstrating the excellent potential of the OADE configuration.

REFERENCES

1. M. Orefice and P. Pirinoli, Dual reflector antenna with narrow broadside beam for omnidirectional coverage, Electron Lett 29 (1993), 2158–2159.
2. A.G. Pino, A.M.A. Acuna, and J.O.R. Lopez, An omnidirectional dual-shaped reflector antenna, Microwave Opt Technol Lett 25 (2000), 371–374.
3. J.R. Bergmann, F.J.V. Hasselmann, and M.G.C. Branco, A single-reflector design for omnidirectional coverage, Microwave Opt Technol Lett 24 (2000), 426–429.
4. F.J.S. Moreira and A. Prata, Jr., Generalized classical axially symmetric dual-reflector antennas, IEEE Trans Antennas Propagat 49 (2001), 547–554.
5. K.A. Iskander, L. Shafai, A. Frandsen, and J.E. Hansen, Application of impedance boundary conditions to numerical solution of corrugated circular horns, IEEE Trans Antennas Propagat AP-30 (1982), 363–372.

MICROWAVE MONOLITHIC PHASE SHIFTER FOR OPTICAL TRANSMISSION AT 40 Gb/s

S. Bosse,[1] L. Billonnet,[1] B. Jarry,[1] H. Jallageas,[1] F. Blache,[2] and W. Mouzannar[2]

[1] IRCOM UMR C.N.R.S. n°6615
University of Limoges
123, Avenue A. Thomas
87060 Limoges Cedex, France

[2] Alcatel CIT, OPTO+
Route de Nozay
F-91 460 Marcoussis, France

Received 19 July 2003

ABSTRACT: *This paper deals with a design technique for an integrated planar phase shifter on GaAs substrate at millimetre-wave frequencies for optical transmission applications at 40 Gb/s. We numerically show how an amplifier can be adequately associated with a nonconstant magnitude phase shifter to avoid a magnitude modulation of the optical signal when tuning the phase shift.* © 2004 Wiley Periodicals, Inc. Microwave Opt Technol Lett 40: 254–258, 2004; Published online in Wiley InterScience (www.interscience.wiley.com). DOI 10.1002/mop.11345

Key words: *integrated planar phase shifter; GaAs substrates; optical transmissions*

1. INTRODUCTION

Transmission by optical fiber for submarine connections is an important aspect of high-rate systems. The RZ coding of optical impulses of the soliton type is used in these transmissions. The Mach–Zehnder (MZ) modulator on InP is an adequate component for synchronous regeneration of these impulses [1]. It presents two optical ports (input and output) and two RF ports used here for soliton impulse regeneration. At the two RF ports of the modulator, the signal phase must be equal. At 40 Gb/s, it is difficult to precisely estimate the equivalent electrical length at these ports. One solution to the problem is to add a phase shifter at one RF port as an access in order to adjust the RF signals in phase (Fig. 1).

An identical problem is present in pulse generation based on electro-absorption modulators (EAM) on InP. RF signals have to be injected in phase at the inputs of these modulators through the use of phase shifters (Fig. 2).

For our synchronisation criterion, the phase shifter must perform a 45° continuous-phase shift without any gain variation at a single frequency (here, at 41.5 GHz). Considering manufacturing and assembly drift parasitics (for example, uncertainty regarding

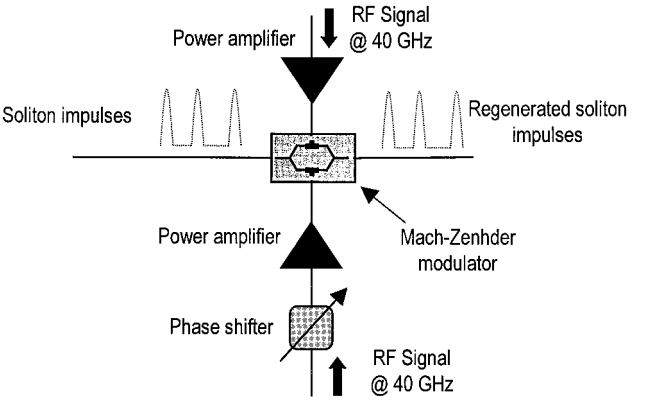

Figure 1 Use of a phase shifter for optical-impulse regeneration

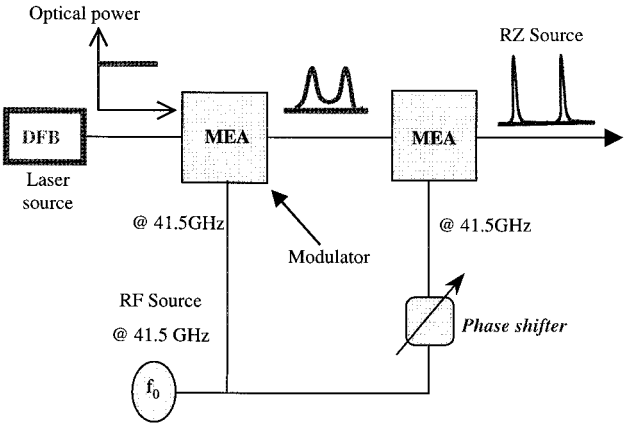

Figure 2 Use of a phase shifter for optical-impulse generation